**Kimberley C. W. Wang**[1]
School of Human Sciences,
The University of Western Australia,
Crawley 6009, Western Australia, Australia;
Telethon Kids Institute,
The University of Western Australia,
Perth 6009, Western Australia, Australia
e-mail: kimberley.wang@uwa.edu.au

**Amy Y. Chang**
School of Human Sciences,
The University of Western Australia,
Crawley 6009, Western Australia, Australia

**J. Jane Pillow**
School of Human Sciences,
The University of Western Australia,
Crawley 6009, Western Australia, Australia;
Centre for Neonatal Research and Education,
Medical School,
The University of Western Australia,
Perth 6009, Western Australia, Australia;
King Edward Memorial Hospital,
Subiaco 6008, Western Australia, Australia

**Béla Suki**
Department of Biomedical Engineering,
Boston University,
Boston, MA 02215

**Peter B. Noble**
School of Human Sciences,
The University of Western Australia,
Crawley 6009, Western Australia, Australia;
Centre for Neonatal Research and Education,
Medical School,
The University of Western Australia,
Perth 6009, Western Australia, Australia

# Transition From Phasic to Tonic Contractility in Airway Smooth Muscle After Birth: An Experimental and Computational Modeling Study

*Fetal airway smooth muscle (ASM) exhibits phasic contractile behavior, which transitions to a more sustained "tonic" contraction after birth. The timing and underlying mechanisms of ASM transition from a phasic to a tonic contractile phenotype are yet to be established. We characterized phasic ASM contraction in preterm (128 day gestation), term (~150 day gestation), 1–4 month, 1 yr, and adult sheep (5yr). Spontaneous phasic activity was measured in bronchial segments as amplitude, frequency, and intensity. The mechanism of phasic ASM contraction was investigated further with a computational model of ASM force development and lumen narrowing. The computational model comprised a two-dimensional cylindrical geometry of a network of contractile units and the activation of neighboring cells was dependent on the strength of coupling between cells. As expected, phasic contractions were most prominent in fetal airways and decreased with advancing age, to a level similar to the level in the 1–4 month lambs. Computational predictions demonstrated phasic contraction through the generation of a wave of activation events, the magnitude of which is determined by the number of active cells and the strength of cell–cell interactions. Decreases in phasic contraction with advancing age were simulated by reducing cell–cell coupling. Results show that phasic activity is suppressed rapidly after birth, then sustained at a lower intensity from the preweaning phase until adulthood in an ovine developmental model. Cell–cell coupling is proposed as a key determinant of phasic ASM contraction and if reduced could explain the observed maturational changes.* [DOI: 10.1115/1.4042312]

## 1 Introduction

Smooth muscle in the fetal airway exhibits spontaneous phasic contractions that are identified in a variety of mammals including chickens, rats, guinea pigs, rabbits, dogs, pigs, and humans [1–5]. Phasic contractions occur when the muscle shortens rapidly to produce spontaneous contraction [6]. Such phasic activity of the airway smooth muscle (ASM) was first described more than 80 years ago and is thought to act as a developmental modulator, promoting lung growth through mechanotransduction pathways [7,8]. After birth, ASM produces predominately tonic force [9–11], a sustained contractile response [6], however, phasic ASM activity is also reported in adult animals and humans [11,12]. No data exist on when and to what extent ASM transitions from a phasic to a tonic contractile phenotype.

Compared with ASM contraction prior to birth, the functional significance (if any) of phasic ASM contraction after birth is less clear [13]. Peristaltic ASM movements to facilitate the movement of air and/or mucus from the lung have been proposed but remain disputed [14,15]. In the context of disease, the "postnatal reversion to prenatal phenotype hypothesis" attributes spontaneous bronchoconstriction in asthmatic patients to a phasic pattern of ASM contraction, albeit over a longer time-scale than in the prenatal lung [7]. That is, the expression of a phasic ASM phenotype in the airways of subjects with asthma may contribute to clinical symptoms and airflow limitation.

Physiological determinants of phasic smooth muscle contraction are well studied [16,17]. Phasic smooth muscle activity is typically more distinctive in single-unit musculature such as esophageal and intestinal smooth muscle where action potentials are generated [18]. Onset of phasic activity in ASM is not clearly understood but circumferential waves of calcium oscillations are documented in mature ASM [19,20]. While the frequency of calcium oscillation increases the amplitude of ASM contraction, the contractile response is predominantly tonic rather than phasic in nature [21]. There is evidence of spontaneously activated cells within the ASM layer [22] and also of gap junctions [23] that may propagate an activation signal. The presence of spontaneously active cells and gap junctions, therefore, provides a theoretical mechanistic framework for the emergence of phasic ASM contraction at any stage of life.

In this study, we examined phasic activity of pre- and postnatal ASM using an ovine developmental model. Mechanisms of phasic ASM contraction were investigated using a computational model of ASM force production and narrowing based upon probability of cell activation and cell–cell interactions. We further question to what extent the phasic contraction of ASM might be similar to a wave propagating through the airway wall. Findings demonstrate

[1]Corresponding author.

Manuscript received August 29, 2018; final manuscript received December 11, 2018; published online February 8, 2019. Assoc. Editor: Chun Seow.

that the intensity of phasic ASM contraction reduces rapidly after birth, which is consistent with a fall in spontaneous ASM cell activation and/or "coupling" between cells.

## 2 Materials and Methods

**2.1 Animals and Ethics Approval.** All animal experiments conformed to institutional ethics and animal care unit regulations and were approved by the Animal Ethics Committee (RA/3/100/1368), University of Western Australia. Five sheep groups were studied: preterm fetal lambs delivered via caesarean section at 128 day gestation ($n = 10$); term (~150 day gestation, $n = 8$); 1–4 month lambs ($n = 13$); and sexually mature young adult (1 yr, $n = 6$) and adult (5 yr, $n = 8$) sheep. All animals were euthanized by intravenous sodium pentobarbitone overdose (150 mg $kg^{-1}$) and subsequently exsanguinated. The lungs were removed and transported on ice for subsequent laboratory dissection.

**2.2 Airway Segment Preparation.** Bronchial segments were dissected, free of lung parenchyma, from the main stem bronchus of the right lower lobe, with all side branches ligated with surgical silk. The bronchial segments were cannulated at both ends and mounted horizontally in the organ bath containing gassed Krebs solution at 37 °C [24–26]. The length of the bronchial segment in the organ bath was stretched to 120% of the relaxed length, to account for the recoil in length after dissection (determined in preliminary experiments).

The proximal end of the airway was connected to a reservoir filled with Krebs solution, which was used to flush the lumen between experiments. The reservoir was set at a height that would exert 5 cm $H_2O$ of transmural pressure ($P_{tm}$) on the airway wall. The distal end of the airway was connected to a servo-controlled syringe pump with pressure feedback as previously described [25,26]. All protocols were performed in a closed system, created by closure of a tap between the airway and the Krebs solution reservoir, and via the pressure-controlled syringe pump maintained a constant $P_{tm}$ of 5 cm $H_2O$ by modifying lumen volume. Cyclical changes in lumen volume under constant pressure were used as an index of phasic ASM contraction. The system was leak-tested prior to each experiment and compliance was negligible.

**2.3 Experimental Protocol.** After dissection and mounting, airways were equilibrated for 1 h under static $P_{tm}$ of 5 cm $H_2O$, to simulate functional residual capacity in vivo. The Krebs solution in the organ bath was replaced every 10 min throughout the experiment to remove metabolites. Viability of the tissue was subsequently confirmed by parasympathetic nerve stimulation via electric field stimulation (60 V, 3 ms, 30 Hz for 10 s). Following 5 min recovery, airway segments were exposed to a single dose of acetylcholine (ACh; $10^{-4}$ M) and washed out. This stimulation protocol (agonist and electrical) is a conventional approach to equilibrate the airway to the new organ bath conditions [24].

Spontaneous phasic activity was examined up to ~2 h after equilibration. Airways were fully relaxed to theophylline ($10^{-2}$ M) at the end of the experiment and the volume of the airway at 5 cm $H_2O$ ($V_5$) was determined by withdrawal of the syringe until closure [27]. Three parameters of phasic activity were assessed: frequency (the number of contractions/min), amplitude (the peak to trough volume change expressed as a percentage of $V_5$), and intensity (the product of fractional amplitude and frequency; $\Delta V/V_5 \times$ contractions/min). The SD of intensity was also computed for each animal.

**2.4 Computational Model of Airway Contraction.** To aid the interpretation of the experimental data, we developed a simple computational model (Fig. 1) of an airway segment composed of identical ASM cells arranged in a rectangular array of size $N_x$ by $N_y$, in the horizontal and vertical directions, respectively. The model has circular boundary conditions in the $y$ direction so that the sheet can be considered as a tube. We assume that each cell has the ability to contract with a baseline probability per unit time denoted by $p_a$. When contraction occurs, the cell is in the active state of duration $T_a$ followed by a refractory state of duration $T_r$ and the cell cannot be activated over this period. In addition to the spontaneous activity, cells interact with their neighbors, which alter their total probability $p$ of being in the active state. The cell–cell interactions are taken into account by increasing $p$ locally for a cell if any of its four neighbors are in the active state. Thus, if a cell is in the relaxed state, the probability that it becomes active is

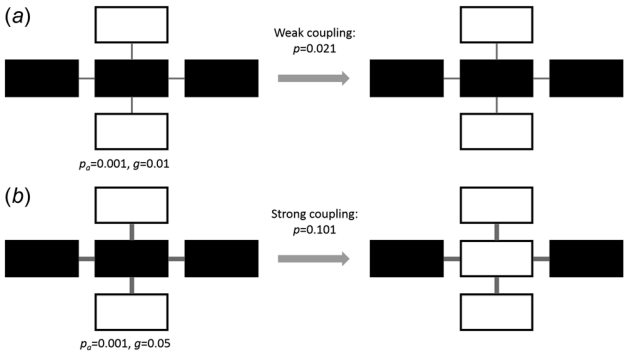


**Fig. 1 Schematic representation of the probabilistic update of cell state in the network model. White and black blocks represent active and relaxed cells, respectively. The gray lines linking the central cell to its four neighbors represent the coupling strength ($g$) with the line thickness being proportional to coupling strength. The probability of spontaneous activation of the middle cell is $p_a = 0.001$. (*a*) The value of $g$ is small and this weak coupling only slightly increases the total probability of the cell becoming active, which is $p = p_a + 2 \times g = 0.021$. In this example, the cell is not activated. (*b*) The value of $g$ is larger and strong coupling significantly increases the total probability of the cell becoming active which is $p = p_a + 2 \times g = 0.101$ resulting in an activation of the cell.**

$$p = p_a + g_l + g_r + g_t + g_b \tag{1}$$

where $g_l$, $g_r$, $g_t$, and $g_b$ denote the strength of interaction of the cell with its left, right, top, and bottom neighbor, respectively. If a neighbor cell is in the refractory state, the corresponding interaction is subtracted from $p$. When the interaction strengths are negligible, cells can become spontaneously active with probability $p_a$. Additionally, we assume that a "neighbor-activated" cell will also attempt to synchronize its active cycle to the average neighbor activation by setting its clock to $q = (t_1 + t_2 + t_3 + t_4)/4$, where $t_1$, …, $t_4$ are between 1 and $T_a$ and describe the clock state of each four neighbors. Therefore, a cell in the relaxed state will transition to the average active state of its neighbors with probability $p$.

The model is assumed to be under isobaric conditions with a baseline stiffness $K_b$. When a transmural pressure $P_{tm}$ is applied across the wall, the volume of the airway at baseline is $V_b = P_{tm}/K_b$. When ASM cells contract, the pressure is maintained at $P_{tm}$, but the volume decreases from $V_b$ to $V$ and the expelled volume, $\Delta V = V_b - V$, is equivalent to what is measured experimentally. Thus, the goal is to compute $\Delta V$, or the relative change in volume, $\Delta V/V_b$, as a function of the contractile state of all cells in the model and age.

To determine $\Delta V$ during contraction, we calculate it as

$$\Delta V = \frac{P_{tm}}{K_b} - \frac{P_{tm}}{K} \tag{2}$$

where $K$ is the wall stiffness that is determined by the active and relaxed ASM cells in the wall, and $K > K_b$. To relate $K_b$ and $K$ to single cell level properties, we note that a computational network

model of a single ASM cell suggested that cell stiffness ($k$) increases linearly with the magnitude of contractile force $f_c$ [28]. In our network model, each cell is modeled accordingly as follows:

$$k = (1 + \alpha f_c)k_b \tag{3}$$

where $k_b$ is the baseline stiffness of a single cell in the absence of contraction and $\alpha$ is a proportionality constant to nondimensionalize force. For simplicity, we allow $f_c$ to take only two values, 0 in the relaxed state or 1 in the activated state. To scale the individual ASM cell stiffness to the entire wall, we further assume that cells are mechanically connected in the circumferential direction as springs in series, each having a $k$ described in Eq. (3), and because the model is axially constrained, neighboring circumferential rings do not interact due to contraction. Consequently, $K$ is the sum of the stiffness values of $N_x$ rings in parallel each composed of $N_y$ springs in series

$$K = \sum_{m=1}^{N_x}\left[\sum_{n=1}^{N_y}\frac{1}{(1 + \alpha f_c(m,n))k_b}\right]^{-1} \tag{4}$$

where $f_c(m, n)$ is the time varying contractile force (0 or 1) of the $n$th cell in the $m$th ring that depends on $p$. Note that if all cells are relaxed ($f_c(m, n) = 0$), Eq. (4) reduces to the passive stiffness of the wall, $K_b = (N_x/N_y)k_b$. Furthermore, by replacing $f_c(m, n)$ in Eq. (4) with its average value $\langle f_c \rangle$, which is related to the fraction of activated cells, Eq. (4) can be simplified to the following:

$$K = (1 + \alpha\langle f_c\rangle)k_b\frac{N_x}{N_y} = (1 + \alpha\langle f_c\rangle)K_b \tag{5}$$

Equation (5) suggests that wall stiffness during contraction is proportional to the baseline stiffness and increases nearly linearly with the average contractile force which is consistent with the experimental results seen at the whole airway level [29]. Finally, substituting the right-hand side of Eq. (5) to Eq. (2), we obtain the relative change in volume as

$$\frac{\Delta V}{V_b} = \frac{\alpha\langle f_c\rangle}{1 + \alpha\langle f_c\rangle} \tag{6}$$

Equation (6) provides the link between the relative volume displaced by the airway at isobaric conditions and the average microscopic force of the ASM cell.

In the computational simulations, Eq. (4) was calculated and substituted into Eq. (2) to predict relative volume changes during a simulation including 2,500,000 time steps for the following parameter combinations using MATLAB R2018a. The value of $T_a$ was set to 100, while $T_r$ was varied between 1 and 100. Cell–cell interactions were assumed to be isotropic with $g = g_l = g_r = g_t = g_b$ and the value of $g$ was varied between 0.002 and 0.256 for several values of $p_a$ ranging from 0.0005 to 0.05. The parameters $T_a$ and $T_r$ are completely arbitrary, and the $g$ values are probabilities. These parameters were chosen after initial testing of the model followed by a broad sweep in the parameter space. The peaks in $\Delta V/V_b$ were identified with a peak detection algorithm from which we computed the mean and SD of amplitudes, contraction frequency defined as the inverse of the time between peaks and the intensity defined as the product of amplitude and frequency.

**2.5 Statistics.** Normally distributed data were analyzed using one-way analysis of variance, and all pairwise multiple comparison using SIGMAPLOT (version 13.0, Chicago, IL). If data could not be normalized, one-way analysis of variance on ranks was used (SIGMAPLOT). Data from the different age groups are expressed as mean ± SEM or median ± interquartile range (IQR) (GRAPHPAD PRISM, version 5.0; GraphPad Software, La Jolla, CA). Differences between groups were considered statistically significant at $P < 0.05$.

**Table 1 Group characteristics**

| Group | Sex (M:F) | Body mass (kg) |
|---|---|---|
| Fetal (128 d gestation) | 7:3 | 3.3 ± 0.4 |
| Term (150 d gestation) | 5:3 | 4.8 ± 0.3 |
| 1–4 month lambs | 9:4 | 22.6 ± 3.3 |
| 1-yr-old sheep | 6:0 | 39.0 ± 1.2 |
| 5-yr-old sheep | 0:8 | 66.6 ± 3.7 |

Data are mean ± SEM. M, male; F, female; and d, days. Body mass means were calculated based on $n = 8$, $n = 11$, and $n = 6$ for fetal, 1–4 month lambs, and 5-yr-old sheep, respectively, since weights of some animals were not available. Other groups had complete data.

**Table 2 Length, volume, and generation of bronchial segments**

| Group | Length (mm) | Volume ($\mu$L) | Generation |
|---|---|---|---|
| Fetal (128 d gestation) | 22.9 ± 2.1 | 486.8 ± 45.0 | 1–10 |
| Term (150 d gestation) | 30.0 ± 0.6 | 581.5 ± 35.5 | 4–10 |
| 1–4 month lambs | 29.2 ± 0.7 | 885.7 ± 84.7[a,b] | 9–12 |
| 1-yr-old sheep | 31.0 ± 0.5[a] | 1103.9 ± 59.5 [a,b] | 11–13 |
| 5-yr-old sheep | 28.9 ± 1.6 | 1208.2 ± 174.5 [a,b] | 11–14 |

Length is the stretched airway length in the organ bath. Volume is lumen volume at 5 cm $H_2O$ after theophylline. Data are mean ± SEM. Generation (mode for each distal and proximal end of the segment) was determined by counting the number of side-branches along the mainstem bronchus with trachea defined as Generation 0. Generation was not recorded for 3 airways in the fetal group.
[a]Significantly different from fetal ($P < 0.05$).
[b]Significantly different from term ($P < 0.05$), d: days.

## 3 Results

**3.1 Animal and Bronchial Segment Characteristics.** The sex and mass of animals are shown in Table 1. Length, volume, and generation of bronchial segments are shown in Table 2. Immature airways were taken from a more proximal location of the main stem bronchus and had a lower lumen volume despite comparable lengths.

**3.2 Phasic Airway Smooth Muscle Contraction in Sheep Bronchi.** Example traces of spontaneous phasic ASM contraction are provided in Fig. 2. Phasic activity was observed in all age groups before and after birth, but was most prominent in fetal and term groups, with a pronounced decrease in older animals. The amplitude of spontaneous volume oscillation in the 1–4 month old lamb group fell substantially compared with the term group ($P = 0.045$; Fig. 3(*a*)). Frequency of spontaneous phasic contraction was significantly lower in 1- and 5-yr-old sheep compared with the fetal group ($P < 0.001$; Fig. 3(*b*)). The frequency of spontaneous phasic contraction in 1-yr-old sheep was also lower compared with the term group ($P = 0.038$; Fig. 3(*b*)). The intensity of phasic activity, expressed as a product of amplitude and frequency, was greatest in fetal and term groups compared with 1–4 month old lamb, 1- and 5-yr-old sheep ($P < 0.001$; Fig. 3(*c*)). The duration of phasic activity (median ± IQR) varies within and between groups, with the duration higher in lamb ($P = 0.006$), 1- ($P < 0.001$) and 5-yr-old ($P = 0.002$) sheep compared with the fetal group: fetal, 4.9 [1.7–8.7] min; term, 10.9 [5.8–25.2] min; lamb, 14.4 [8.7–25.6] min; 1-yr-old sheep, 37.4 [23.9–76.1] min; 5-yr-old sheep, 18.2 [13.7–27.0] min.

**3.3 Modeling the Transition From Phasic to Tonic Contraction.** Our computational model closely mimicked the characteristics of spontaneous phasic contraction observed in

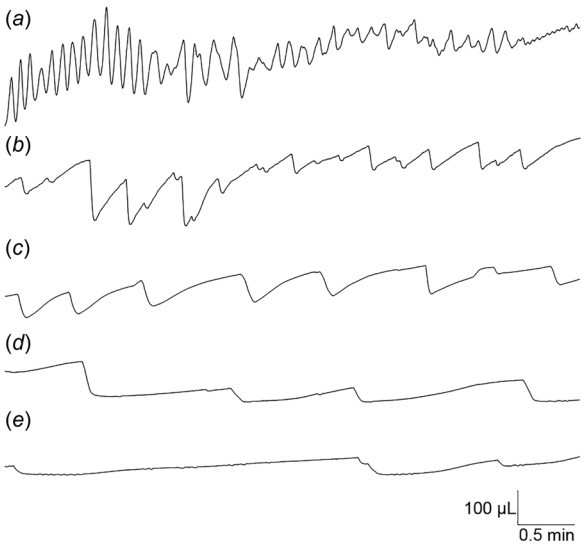


**Fig. 2 Example traces of phasic airway smooth muscle contraction in sheep. Downward deflections represent contraction (reduced volume), and upward deflections relaxation (increased volume). (*a*) fetal; (*b*) term; (*c*) 1–4 month lamb; (*c*) 1-yr-old sheep (*d*); and 5-yr-old sheep (*e*).**

sheep bronchi and allowed us to empirically test the importance of the parameters involved in the transition of ASM with maturation. The model synchronized phasic contractions when the spontaneous activation parameter was set to a large value ($p_a = 0.05$) with medium cell-cell interaction strength ($g = 0.05$; Figs. 4(*a*)–4(*c*), Supplementary Video 1, which is available under the "Supplemental Materials" tab for this paper on the ASME Digital Collection). In contrast, the model displayed sporadic contractions with isolated spikes that generated wave propagation of cellular contraction for low spontaneous activation ($p_a = 0.000002$) coupled with strong cell–cell interactions ($g = 0.1$; Figs. 4(*d*)–4(*f*), Supplementary Video 2, which is available under the "Supplemental Materials" tab for this paper on the ASME Digital Collection).

Based on preliminary simulation results, we find that the three parameters broadly involved in the generation of phasic contractions are cell excitability ($p_a$), $T_r$, the refractory period, and the strength of coupling between neighboring cells ($g$). In the absence of cell coupling ($g = 0$), we observe a constant displaced volume due to contraction, even when $g = 0$ is accompanied by high $p_a$ and $T_r$ (Fig. 5(*a*), Supplementary Video 3, which is available under the "Supplemental Materials" tab for this paper on the ASME Digital Collection). A variety of behaviors including oscillations are observed when $T_r$ is large but $p_a$ and $g$ are low, as the model produces isolated clusters of active cells, but these clusters do not interact (Fig. 5(*b*)). The most interesting behavior is the sporadic oscillations with large $T_r$, but very low $p_a$ and medium $g$ (Fig. 5(*c*)). The sporadic oscillations shown in Fig. 5(*c*) suggest that the system rarely reaches the threshold to initiate a measurable contraction because $p_a$ is low. However, synchronization occurs (albeit suboptimal) if a low $p_a$ is combined with a relatively strong $g$ to produce a more coherent interaction among activated clusters, leading to a propagating contraction wave.

The decrease in phasic activity with age as seen in the sheep bronchi (Fig. 3) can be replicated by the model through gradual reduction in cell coupling. When $g$ was set to decrease with age ($g = 1/\text{age}$), $g$ but not $p_a$ appears to impact the final amplitude (Fig. 6(*a*)), frequency (Fig. 6(*b*)), and intensity (Fig. 6(*c*)) of phasic contraction. Phasic contractions can be obtained with very low excitability ($p_a = 0.0005$) and strong $g$; however the reverse, that is, high cell excitability ($p_a = 0.004$) with weak $g$, will not produce phasic oscillation. This finding indicates that the propagation

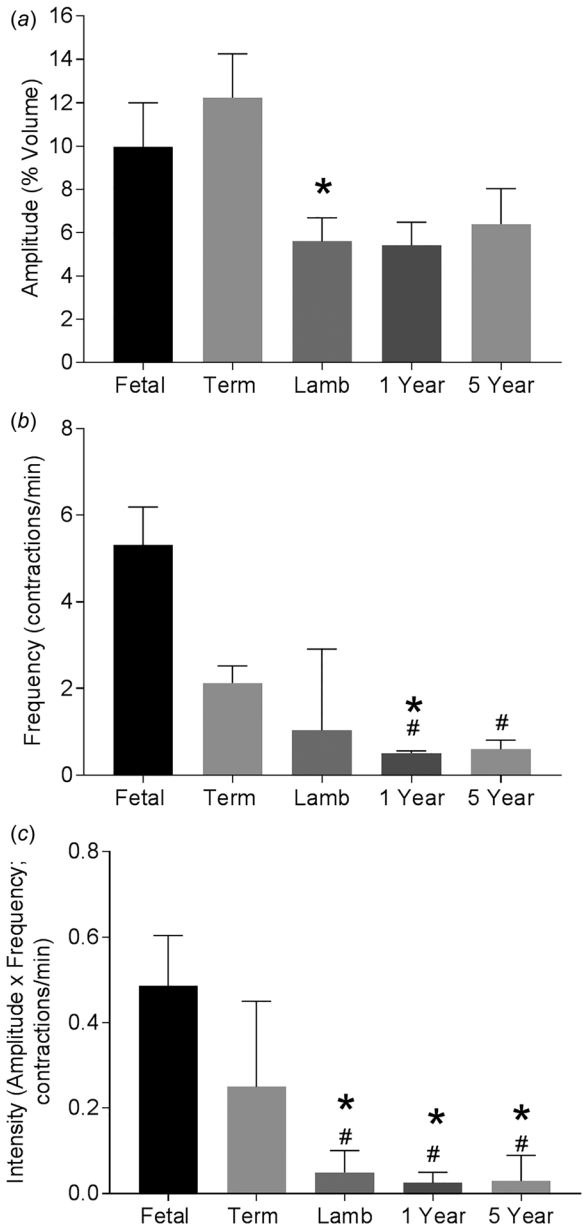


**Fig. 3 Spontaneous phasic contraction of ASM in sheep. Amplitude (*a*), frequency (*b*), and intensity (*c*) of fetal, term, lamb, 1 yr and 5 yr sheep. Data are mean ± SEM. #Significantly different from fetal ($P < 0.05$); *Significantly different from term ($P < 0.05$).**

of spontaneous contractions and the production of volume oscillation are primarily determined by $g$.

The SD of intensity of ASM contraction measured in the sheep bronchi was significantly reduced in the 1–4 month lamb, 1- and 5-yr-old sheep compared with the fetal or term groups ($P < 0.05$; Fig. 7(*a*)). Our computational model also reproduced this feature of the data; indeed, the model-predicted SD of the intensity decreased with age (Fig. 7(*b*)).

## 4 Discussion

This study examined phasic activity from late gestation to adulthood using an ovine developmental model. Spontaneous phasic activity measured in isolated bronchial segments in vitro was most prominent in fetal airways. Some phasic activity was still observed in adult animals although intensity of this activity reduced markedly after birth. The experimentally identified

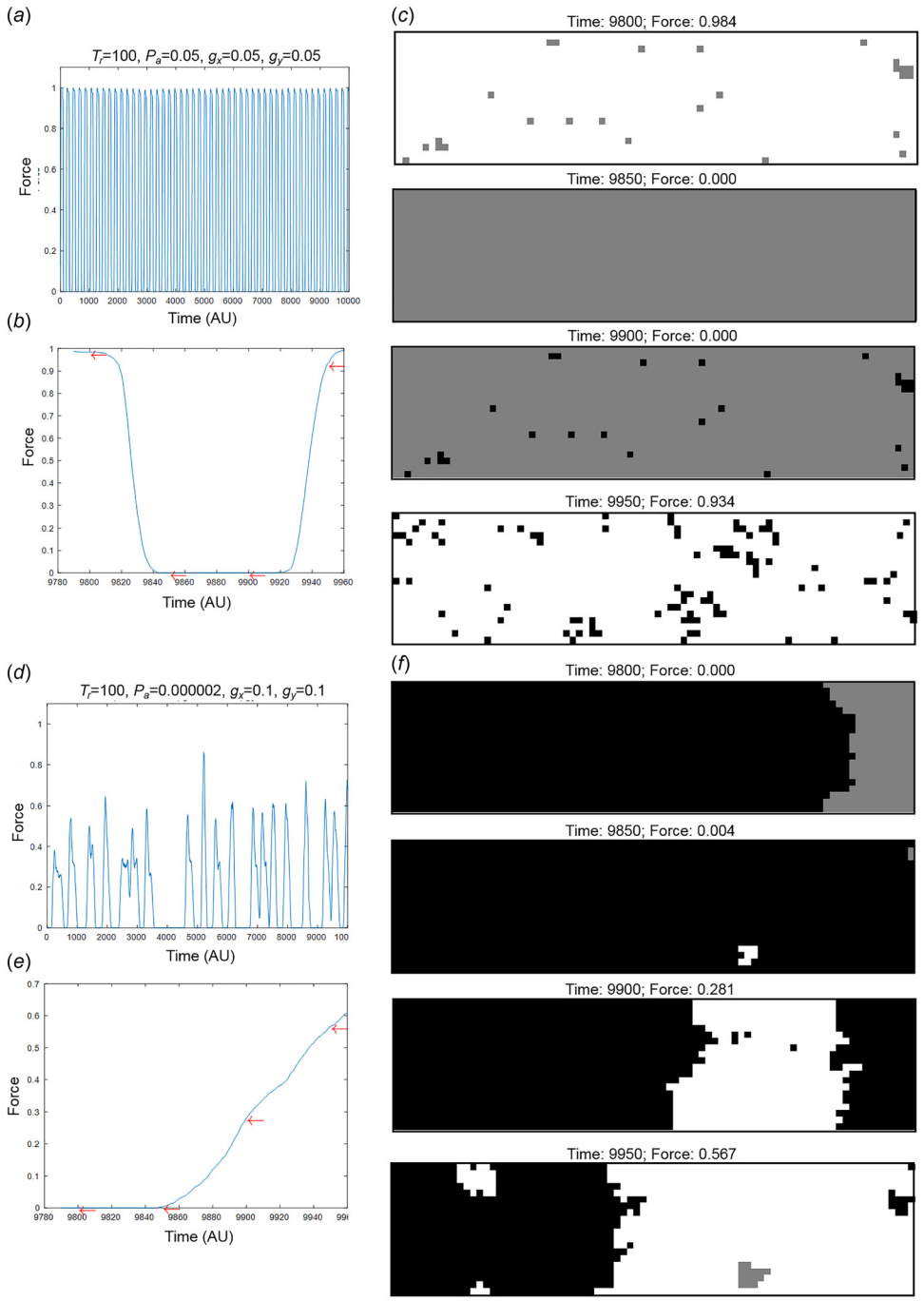


**Fig. 4 Simulated contractile activity. Complete synchronization of phasic contractions, illustrated by force oscillations generated by the computational model ($T_r = 100$ simulations; $p_a = 0.05$; $g = 0.05$; contraction time = 100 (*a*)). Zoomed-in view of the phasic contractions shown in panel a (*b*). Model configurations corresponding to the contraction shown in panel b (*c*). Sporadic contraction with wave propagation of phasic contractions, illustrated by force oscillations generated by the computational model ($T_r = 100$ simulations; $p_a = 0.000002$; $g = 0.1$; contraction time = 100 (*d*)). Zoomed-in view of the phasic contractions shown in panel d (*e*). Model configurations corresponding to the contraction shown in panel e (*f*). The arrows represent different stages of phasic contraction. $T_r = 100$ simulations; $p_a = 0.05$; contraction time = 100. Black pixel, resting and excitable cells; white pixel, active cells (contracting); gray pixel, resting and nonexcitable cells (refractory). $T_r$, time period for refractory state; $p_a$, cell excitability; $g$, strength of coupling between neighboring cells; AU, arbitrary units.**

transition from phasic to tonic ASM contraction was simulated in a computational model by gradually reducing the strength of cell to cell coupling.

The precise mechanism underlying the transition from phasic to tonic ASM contraction after birth is not known, but may intuitively reflect disruption of temporal and spatial distribution of ASM activation events. Phasic contraction in other smooth muscle types, involves spontaneous depolarization of pacemaker cells and the propagation of action potential via gap junctions to neighboring cells [30]. Pacemaker cells in the airway are not well

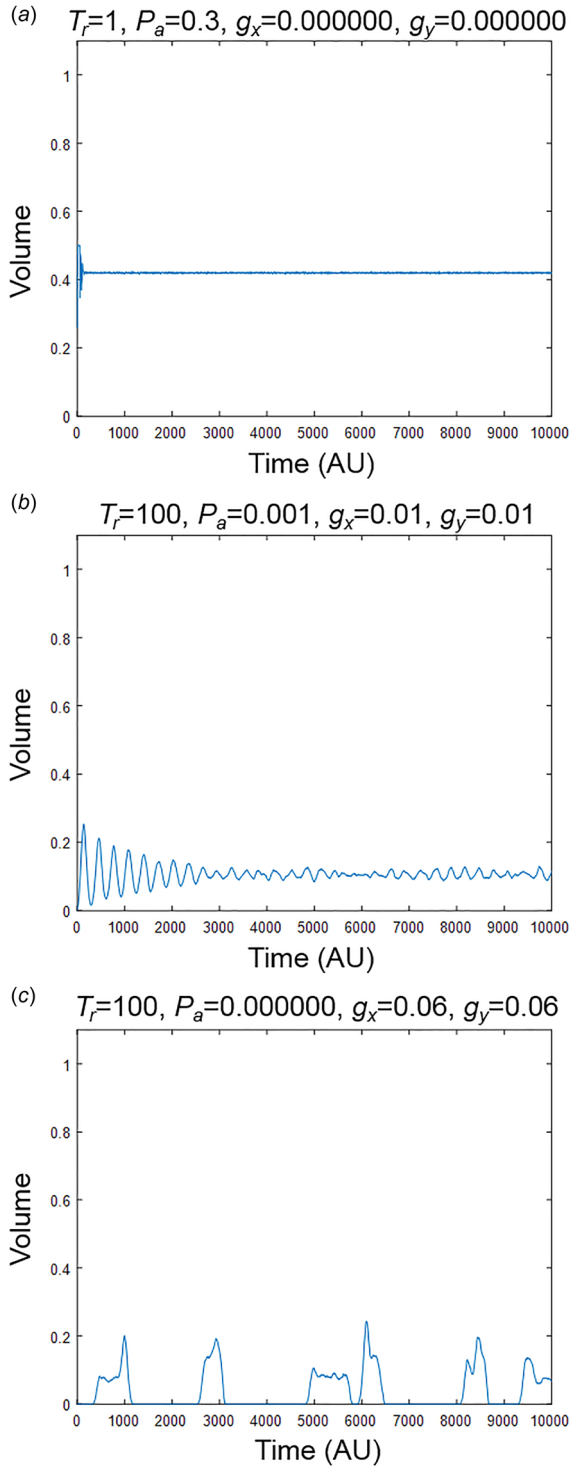


**Fig. 5 Simulated volume displacement. The absence of cell coupling with high $p_a$ and $T_r$ (*a*), large $T_r$ with low $p_a$ and $g$ (*b*), and large $T_r$, but very low $p_a$ and medium $g$ (*c*) produces different contractile behavior. $T_r$, time period for refractory state; $p_a$, cell excitability; $g$, strength of coupling between neighboring cells; AU, arbitrary units.**

established; however, some studies have suggested that spontaneous rhythmic activities are generated primarily from the proximal right lung [7,31]. Gap junctions identified in the airway presumably allow for coordinated phasic contractions [8,32].

We, therefore, devised a computational model of ASM force generation and subsequent airway narrowing to examine a potential mechanism facilitating phasic to tonic ASM transition. The two most important parameters in the model were the probability of cell activation and the strength of cell to cell coupling, which correspond, respectively, to spontaneous muscle activation and gap junctions. The degree of cell to cell coupling ($g$) appears to play a critical role in the generation of phasic activity, since phasic activity could be mimicked with very low cell excitation as long as cell to cell coupling was strong (Figs. 4(*d*)–4(*f*)). These results suggest that the transition from a phasic to a tonic ASM phenotype with maturation could be simulated by gradually decreasing the strength of cell to cell coupling. If we assume that changes in coupling in the model are reflective of ASM gap junctions, a reduction in gap junction expression with age is a testable hypothesis that has a basis in other tissue types. For example, endothelial gap junctions are maximally expressed in rat aorta at birth, with gap junction expression declining within the first week of life [33].

The probability of cell activation ($p_a$) was the other key parameter in the model. Cyclical activation of ASM cells is not purely restricted to intrinsic pacemaker activity, but may instead be pharmacologically mediated. For example, charybdotoxin-induced oscillatory contraction in guinea pig airways is regulated by activation of the cyclooxygenase two enzyme and downstream production of prostaglandins [34]. In murine airways, tetraethylammonium chloride induced oscillations in intracellular

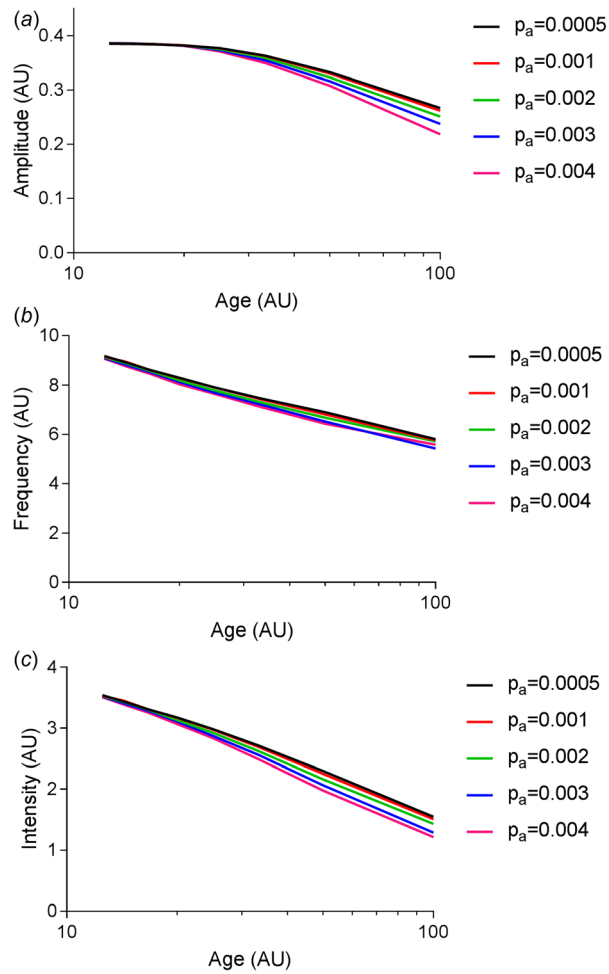


**Fig. 6 Decreased cell coupling as a surrogate for the effect of age on phasic contraction. Age (marker for strength of cell–cell interactions) was manipulated to determine its effect on the amplitude (*a*), frequency (*b*), and intensity (*c*) of phasic contractions. $T_r$ = 10 simulations; contraction time = 100. $T_r$, time period for refractory state; $p_a$, cell excitability; AU, arbitrary units.**

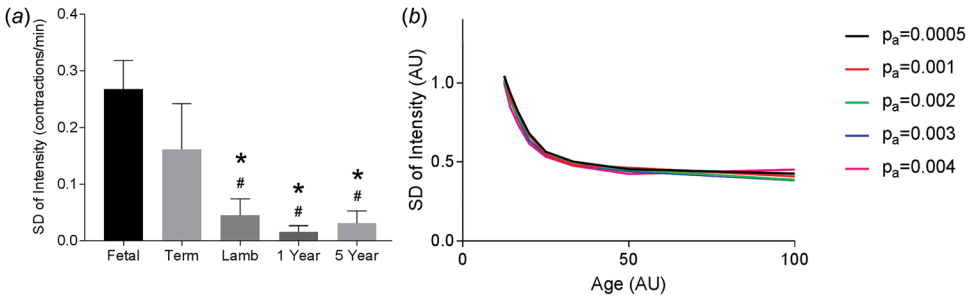


**Fig. 7 SD of the intensity of phasic contraction measured in sheep bronchi (*a*) or simulated (*b*). Values are median ± IQR. $T_r = 10$ simulations; contraction time = 100. #Significantly different from fetal ($P < 0.05$); *Significantly different from term ($P < 0.05$). $T_r$, time period for refractory state; $p_a$, cell excitability; AU, arbitrary units.**

$Ca^{2+}$ and force were produced cooperatively by L-type voltage-dependent $Ca^{2+}$ channels, voltage-dependent $Na^{+}$ channels, $Ca^{2+}$-activated $Cl^{-}$ channels, $Na^{+}$–$Ca^{2+}$ exchanger, $Na^{+}/K^{+}$ ATPase, release from $Ca^{2+}$ stores mediated by inositol (1,4,5)-trisphosphate, and extracellular $Ca^{2+}$ [35]. Whether phasic ASM contraction occurs appears dependent on the frequency of $Ca^{2+}$ oscillation, wherein frequencies exceeding 40 cycles/min produce sustained (tonic) contraction [30] and phasic ASM contraction at much lower frequencies [31]. The frequency of contraction observed in the present study ranged from 0.5 to 5.3 contractions/min (Fig. 3) in sheep airways which in the future should be compared with direct measurements of intracellular $Ca^{2+}$ over the same time period. Irrespectively, the model parameter ($p_a$) should not be considered a specific representation of pacemaker activity, but any pathway that leads to spontaneous cell activation and thereafter latency.

Despite its overriding simplicity, our computational model exhibited a rich set of behaviors ranging from fully deterministic synchronized waves (Figs. 4(*a*)–4(*c*), Supplementary Video 1, which is available under the "Supplemental Materials" tab for this paper on the ASME Digital Collection), which are similar in part to the contractions in the fetal airway (Fig. 2(*a*)), through more isolated sporadic waves (Figs. 4(*d*)–4(*f*), Supplementary Video 2, which is available under the "Supplemental Materials" tab for this paper on the ASME Digital Collection) somewhat reminiscent to the contractions in the term airway (Fig. 2(*b*)), to a constant level of contraction (Fig. 5(*a*), Supplementary Video 3, which is available under the "Supplemental Materials" tab for this paper on the ASME Digital Collection) that may represent the tonic contraction with slow swings in the adult airway (Fig. 2(*e*)). While the biological mechanism associated with phasic contraction is the average single cell contractility that is responsible for the full airway contractility [31], the mechanism of contraction in our model is wave propagation (Fig. 4). This finding raises the possibility that phasic behavior is a network phenomenon arising from cell–cell interactions, rather than molecular mechanisms of single cell contractions. This idea of network behavior reproduced all of the measured data features, provided the cell–cell interaction parameter $g$ decreased with age. In the absence of relevant data for ASM, we chose the simplest mathematical relation between $g$ and age: $g = 1/\text{age}$. While other forms could be explored, this simple relation produced behavior similar to the data (Fig. 3 versus Fig. 6). As the strength of cell–cell coupling is reduced with age, the probability that an activated cell induces a full wave is also reduced. Hence, both the frequency and amplitude, and hence, the intensity, of the waves decrease with age. It is noteworthy that the model also predicted that the SD of amplitude has a peak (data not shown) because with decreasing age, cell–cell coupling becomes stronger and all waves begin to be synchronized with similar amplitudes. Such a full synchronization is only rarely seen in the experimental data (see first 2 min in Fig. 2(*a*)). Nevertheless, the SD of intensity, being the product of amplitude and frequency, still shows a strong decrease with age, in agreement with the experimental data (Fig. 7).

An improved understanding regarding the physiology of phasic ASM contraction is potentially relevant to the pathogenesis of common obstructive diseases such as asthma. Jesudason draws a creative link between asthma and phasic ASM contraction [7]. Transient airflow limitation, which is a primary characteristic of asthma [36], is conceptually similar to the rhythmic mechanical response associated with phasic ASM contraction. The hypothesis proposed by Jesudason states that reversion to a prenatal ASM phenotype contributes to asthma onset [7]. Given the early life presentation of asthma, we further speculate that phasic ASM contraction may never completely transition in individuals at risk of asthma development. There is now an abundance of evidence to suggest that a number of prenatal factors contribute to asthma development including fetal growth kinetics [37–39], preterm birth [40], and intrauterine infection [41]. Deficits in airway function at birth and in childhood are independent risk factors for the development of asthma [42,43]. Wheezing, an apparent symptomatic expression of airflow limitation, is common in infants [44]. Notably, wheezing phenotypes also include transient wheeze [45] which is perhaps most analogous to phasic ASM contraction. An unanswered question is whether the established associations between adverse events in early life and asthma are mediated by a direct effect on airway function that may include persistence of or regression to phasic ASM contraction.

There are limitations and assumptions in both biological and computational models used in the present study. Sex is a potential confounder, particularly in the older groups. Males were only available in the 1-yr-old group, while 5-yr-old females were studied as these were the mother ewes of the younger groups. Younger groups comprised both male and female lambs. Recent studies have raised the possibility of sex differences in ASM behavior and the role of sex hormones in the etiology of asthma is acknowledged [46]. Indeed, there is a sex-dependent shift in asthma prevalence from childhood to adulthood; the prevalence of asthma is greater in boys than girls during early childhood, but this trend is reversed after puberty [47]. It seems less likely that sex differences will be expressed at the level of the isolated airway in vitro, where normal regulation from external stimuli is lost. For example, while male sex hormones increase airway responsiveness to cholinergic stimulation via a vagus nerve-mediated reflex mechanism, contractile response of isolated tracheal and bronchial ring segments to carbachol are not different between males and females [48]. No obvious differences were observed between males and females in the present study, further, any sex differences cannot explain a decrease in phasic activity with age. Therefore, conclusions drawn from this study are not expected to be different if sex was controlled across groups.

The computational model is a simple statistical model devised to primarily investigate how the assembly of simple contractile units in the presence of varying neighbor interactions behave. We

thus neglected all internal molecular mechanisms that participate in force generation. We also did not specify the nature of cell–cell interactions which might include information flowing through gap junctions, calcium waves, or mechanical force-induced signaling that can lead to cell activation [19,23,49]. For example, when a cell is in the activated state, it may release mediators as well as produce localized force that can affect the activation state of the neighbor cell. These processes may take time which may in part be represented by the period associated with the refractory period $T_r$. Nevertheless, to our knowledge, the ASM cell does not have a refractory period. To test the effect of $T_r$ on model results, we carried out various complementary simulations and found that $T_r = 0$ was not different from $T_r = 1$ suggesting that the refractory period is not an essential component of the model. Another simplification is the assumption that axial forces do not contribute to the expelled volume during a full airway contraction. Finally, the effects of the extracellular matrix were also neglected. Contractile forces can propagate through the collagen fibers to neighboring as well as more distal cells potentially influencing their activation. However, as the extracellular matrix strengthens during maturation [50], its stiffness is expected to increase with potential effects on ASM phenotype and contractility. Despite all the simplicity of our minimal model, it was able to qualitatively reproduce the experimental data. Hence, we believe our minimal model captures some aspects of the transition of a full airway from phasic to tonic contractile phenotype.

## 5 Conclusions

In conclusion, the intensity of phasic activity is greatest in fetal bronchi and while present after birth, decreases with age. Model simulations suggest that changes in cell–cell coupling account for the transition from a phasic to a tonic ASM phenotype which should be further tested in future experimental studies. Owing to the broad similarity in transient airflow obstruction in asthma and phasic ASM contraction activity, abnormalities in the normal phenotypic transition to tonic contraction may be of relevance to asthma pathogenesis.


## Acknowledgment

We would like to thank the assistance of Dr. Siavash A. Noorbakhsh in tissue collection.

## Funding Data

- National Health and Medical Research Council (NHMRC) of Australia (1077791 and 1057514, Funder ID. 10.13039/501100000925).
- National Institutes of Health (HL-11745 and U01 HL-139466, Funder ID. 10.13039/100000002).
- National Health and Medical Research Council Early Career Research Fellowship (1090888, Funder ID: 10.13039/501100000925)
- National Health and Medical Research Council Career Development Fellowship (1045824, Funder ID: 10.13039/501100000925).
- National Health and Medical Research Council Senior Research Fellowship (1077691, Funder ID: 10.13039/501100000925).


## References


[1] Schittny, J. C., Miserocchi, G., and Sparrow, M. P., 2000, "Spontaneous Peristaltic Airway Contractions Propel Lung Liquid Through the Bronchial Tree of Intact and Fetal Lung Explants," Am. J. Respir. Cell Mol. Biol., **23**(1), pp. 11–18.

[2] Lewis, M. R., 1924, "Spontaneous Rhythmical Contraction of the Muscles of the Bronchial Tubes and Air Sacs of the Chick Embryo," Am. J. Physiol. Legacy, **68**, pp. 385–388.

[3] Sollmann, T., and Gilbert, A. J., 1937, "Microscopic Observations of Bronchiolar Reactions," J. Pharmacol. Exp. Ther., **61(3)**, pp. 272–285.

[4] Sorokin, S., 1961, "A Study of Development in Organ Cultures of Mammalian Lungs," Dev. Biol., **3**(1), pp. 60–83.

[5] Parvez, O., Voss, A. M., de Kok, M., Roth-Kleiner, M., and Belik, J., 2006, "Bronchial Muscle Peristaltic Activity in the Fetal Rat," Pediatr. Res., **59**(6), pp. 756–761.

[6] Somlyo, A. V., and Somlyo, A. P., 1968, "Electromechanical and Pharmacomechanical Coupling in Vascular Smooth Muscle," J. Pharmacol. Exp. Ther., **159**(1), pp. 129–145.

[7] Jesudason, E. C., 2009, "Airway Smooth Muscle: An Architect of the Lung?," Thorax, **64**(6), pp. 541–545.

[8] Sparrow, M. P., and Lamb, J. P., 2003, "Ontogeny of Airway Smooth Muscle: Structure, Innervation, Myogenesis and Function in the Fetal Lung," Respir. Physiol. Neurobiol., **137**(2–3), pp. 361–372.

[9] Dai, J. M., Kuo, K. H., Leo, J. M., van Breemen, C., and Lee, C. H., 2006, "Mechanism of ACh-Induced Asynchronous Calcium Waves and Tonic Contraction in Porcine Tracheal Muscle Bundle," Am. J. Physiol. Lung Cell Mol. Physiol., **290**(3), pp. L459–L469.

[10] Zhang, W. C., Peng, Y. J., Zhang, G. S., He, W. Q., Qiao, Y. N., Dong, Y. Y., Gao, Y. Q., Chen, C., Zhang, C. H., Li, W., Shen, H. H., Ning, W., Kamm, K. E., Stull, J. T., Gao, X., and Zhu, M. S., 2010, "Myosin Light Chain Kinase Is Necessary for Tonic Airway Smooth Muscle Contraction," J. Biol. Chem., **285**(8), pp. 5522–5531.

[11] Davis, C., Kannan, M. S., Jones, T. R., and Daniel, E. E., 1982, "Control of Human Airway Smooth Muscle: In Vitro Studies," J. Appl. Physiol. Respir. Environ. Exerc. Physiol., **53**(5), pp. 1080–1087.

[12] Ito, Y., Suzuki, H., Aizawa, H., Hakoda, H., and Hirose, T., 1989, "The Spontaneous Electrical and Mechanical Activity of Human Bronchial Smooth Muscle: Its Modulation by Drugs," Br. J. Pharmacol., **98**(4), pp. 1249–1260.

[13] LaPrad, A. S., Lutchen, K. R., and Suki, B., 2013, "A Mechanical Design Principle for Tissue Structure and Function in the Airway Tree," PLoS Comput. Biol., **9**(5), p. e1003083.

[14] Macklin, C. C., 1929, "The Musculature of the Bronchi and Lungs: A Retrospect," Can. Med. Assoc. J., **20**(4), p. 404.

[15] Mitzner, W., 2004, "Airway Smooth Muscle: The Appendix of the Lung," Am. J. Respir. Crit. Care Med., **169**(7), pp. 787–790.

[16] Horowitz, A., Menice, C. B., Laporte, R., and Morgan, K. G., 1996, "Mechanisms of Smooth Muscle Contraction," Physiol. Rev., **76**(4), pp. 967–1003.

[17] An, S. S., Bai, T. R., Bates, J. H., Black, J. L., Brown, R. H., Brusasco, V., Chitano, P., Deng, L., Dowell, M., Eidelman, D. H., Fabry, B., Fairbank, N. J., Ford, L. E., Fredberg, J. J., Gerthoffer, W. T., Gilbert, S. H., Gosens, R., Gunst, S. J., Halayko, A. J., Ingram, R. H., Irvin, C. G., James, A. L., Janssen, L. J., King, G. G., Knight, D. A., Lauzon, A. M., Lakser, O. J., Ludwig, M. S., Lutchen, K. R., Maksym, G. N., Martin, J. G., Mauad, T., McParland, B. E., Mijailovich, S. M., Mitchell, H. W., Mitchell, R. W., Mitzner, W., Murphy, T. M., Paré, P. D., Pellegrino, R., Sanderson, M. J., Schellenberg, R. R., Seow, C. Y., Silveira, P. S., Smith, P. G., Solway, J., Stephens, N. L., Sterk, P. J., Stewart, A. G., Tang, D. D., Tepper, R. S., Tran, T., and Wang, L., 2007, "Airway Smooth Muscle Dynamics: A Common Pathway of Airway Obstruction in Asthma," Eur. Respir. J., **29**(5), pp. 834–860.

[18] Goyal, R. K., and Chaudhury, A., 2008, "Physiology of Normal Esophageal Motility," J. Clin. Gastroenterol., **42**(5), pp. 610–619.

[19] Berridge, M. J., 2008, "Smooth Muscle Cell Calcium Activation Mechanisms," J. Physiol., **586**(21), pp. 5047–5061.

[20] Sanderson, M. J., Delmotte, P., Bai, Y., and Perez-Zogbhi, J. F., 2008, "Regulation of Airway Smooth Muscle Cell Contractility by Ca2+ Signaling and Sensitivity," Proc. Am. Thorac. Soc., **5**(1), pp. 23–31.

[21] Ressmeyer, A. R., Bai, Y., Delmotte, P., Uy, K. F., Thistlethwaite, P., Fraire, A., Sato, O., Ikebe, M., and Sanderson, M. J., 2010, "Human Airway Contraction and Formoterol-Induced Relaxation Is Determined by Ca2+ Oscillations and Ca2+ Sensitivity," Am. J. Respir. Cell Mol. Biol., **43**(2), pp. 179–191.

[22] Zhuge, R., Bao, R., Fogarty, K. E., and Lifshitz, L. M., 2010, "Ca2+ Sparks Act as Potent Regulators of Excitation-Contraction Coupling in Airway Smooth Muscle," J. Biol. Chem., **285**(3), pp. 2203–2210.

[23] Kuo, K. H., Herrera, A. M., and Seow, C. Y., 2003, "Ultrastructure of Airway Smooth Muscle," Respir. Physiol. Neurobiol., **137**(2–3), pp. 197–208.

[24] Ansell, T. K., McFawn, P. K., McLaughlin, R. A., Sampson, D. D., Eastwood, P. R., Hillman, D. R., Mitchell, H. W., and Noble, P. B., 2015, "Does Smooth Muscle in an Intact Airway Undergo Length Adaptation During a Sustained Change in Transmural Pressure?," J. Appl. Physiol., **118**(5), pp. 533–543.

[25] Noble, P. B., Jones, R. L., Cairncross, A., Elliot, J. G., Mitchell, H. W., James, A. L., and McFawn, P. K., 2013, "Airway Narrowing and Bronchodilation to Deep Inspiration in Bronchial Segments From Subjects With and Without Reported Asthma," J. Appl. Physiol., **114**(10), pp. 1460–1471.

[26] Ansell, T. K., Noble, P. B., Mitchell, H. W., and McFawn, P. K., 2014, "Pharmacological Bronchodilation Is Partially Mediated by Reduced Airway Wall Stiffness," Br. J. Pharmacol., **171**(19), pp. 4376–4384.

[27] Noble, P. B., Jones, R. L., Needi, E. T., Cairncross, A., Mitchell, H. W., James, A. L., and McFawn, P. K., 2011, "Responsiveness of the Human Airway In Vitro During Deep Inspiration and Tidal Oscillation," J. Appl. Physiol., **110**(6), pp. 1510–1518.

[28] Parameswaran, H., Lutchen, K. R., and Suki, B., 2014, "A Computational Model of the Response of Adherent Cells to Stretch and Changes in Substrate Stiffness," J. Appl. Physiol., **116**(7), pp. 825–834.

[29] Noble, P. B., McFawn, P. K., and Mitchell, H. W., 2007, "Responsiveness of the Isolated Airway During Simulated Deep Inspirations: Effect of Airway Smooth Muscle Stiffness and Strain," J. Appl. Physiol., **103**(3), pp. 787–795.
[30] Sanders, K. M., 1996, "A Case for Interstitial Cells of Cajal as Pacemakers and Mediators of Neurotransmission in the Gastrointestinal Tract," Gastroenterology, **111**(2), pp. 492–515.
[31] McCray, P. B., Jr., 1993, "Spontaneous Contractility of Human Fetal Airway Smooth Muscle," Am. J. Respir. Cell Mol. Biol., **8**(5), pp. 573–580.
[32] Daniel, E. E., Kannan, M., Davis, C., and Posey-Daniel, V., 1986, "Ultrastructural Studies on the Neuromuscular Control of Human Tracheal and Bronchial Muscle," Respir. Physiol. Neurobiol., **63**(1), pp. 109–128.
[33] Yeh, H. I., Chang, H. M., Lu, W. W., Lee, Y. N., Ko, Y. S., Severs, N. J., and Tsai, C. H., 2000, "Age-Related Alteration of Gap Junction Distribution and Connexin Expression in Rat Aortic Endothelium," J. Histochem. Cytochem., **48**(10), pp. 1377–1389.
[34] Yagi, Y., Kuwahara, M., and Tsubone, H., 2003, "ChTX Induces Oscillatory Contraction in guinea Pig Trachea: Role of Cyclooxygenase-2 and PGE2," Am. J. Physiol. Lung Cell Mol. Physiol., **284**(6), pp. L104510–L104554.
[35] Xu, H., Zhao, P., Zhang, W. J., Qiu, J. Y., Tan, L., Liu, X. C., Wang, Q., Luo, X., She, Y. S., Zang, D. A., Liu, B. B., Cao, L., Zhao, X. X., Chen, Y. Y., Li, M. Y., Shen, J., Peng, Y. B., Xue, L., Yu, M. F., Chen, W., Ma, L. Q., Qin, G., and Liu, Q. H., 2018, "Generation and Role of Oscillatory Contractions in Mouse Airway Smooth Muscle," Cell. Physiol. Biochem., **47**(4), pp. 1546–1555.
[36] Reddel, H. K., and Levy, M. L., and Global Initiative for Asthma Scientific Committee and Dissemination and Implementation Committee, 2015, "The GINA Asthma Strategy Report: What's New for Primary Care?," NPJ Prim. Care Respir. Med., **25**, p. 15050.
[37] Wang, K. C. W., Larcombe, A. N., Berry, L. J., Morton, J. S., Davidge, S. T., James, A. L., and Noble, P. B., 2018, "Foetal Growth Restriction in Mice Modifies Postnatal Airway Responsiveness in an Age and Sex-Dependent Manner," Clin. Sci., **132**(2), pp. 273–284.
[38] Turner, S. W., Campbell, D., Smith, N., Craig, L. C., McNeill, G., Forbes, S. H., Harbour, P. J., Seaton, A., Helms, P. J., and Devereux, G. S., 2010, "Associations Between Fetal Size, Maternal {Alpha}-Tocopherol and Childhood Asthma," Thorax, **65**(5), pp. 391–397.
[39] Sonnenschein-van der Voort, A. M., Gaillard, R., de Jongste, J. C., Hofman, A., Jaddoe, V. W., and Duijts, L., 2016, "Foetal and Infant Growth Patterns, airway Resistance and School-Age Asthma," Respirology, **21**(4), pp. 674–682.
[40] He, H., Butz, A., Keet, C. A., Minkovitz, C. S., Hong, X., Caruso, D. M., Pearson, C., Cohen, R. T., Wills-Karp, M., Zuckerman, B. S., Hughes, M. E., and Wang, X., 2015, "Preterm Birth With Childhood Asthma: The Role of Degree of Prematurity and Asthma Definitions," Am. J. Respir. Crit. Care Med., **192**(4), pp. 520–523.
[41] Xu, B., Pekkanen, J., Järvelin, M. R., Olsen, P., and Hartikainen, A. L., 1999, "Maternal Infections in Pregnancy and the Development of Asthma Among Offspring," Int. J. Epidemiol., **28**(4), pp. 723–727.
[42] Stern, D. A., Morgan, W. J., Wright, A. L., Guerra, S., and Martinez, F. D., 2007, "Poor Airway Function in Early Infancy and Lung Function by Age 22 Years: A Non-Selective Longitudinal Cohort Study," Lancet, **370**(9589), pp. 758–764.
[43] Owens, L., Laing, I. A., Zhang, G., and Le Souëf, P. N., 2017, "Infant Lung Function Predicts Asthma Persistence and Remission in Young Adults," Respirology, **22**(2), pp. 289–294.
[44] Frey, U., 2001, "Why Are Infants Prone to Wheeze? Physiological Aspects of Wheezing Disorders in Infants," Swiss Med. Wkly., **131**(27–28), pp. 400–406.
[45] Martinez, F. D., Wright, A. L., Taussig, L. M., Holberg, C. J., Halonen, M., and Morgan, W. J., 1995, "Asthma and Wheezing in the First Six Years of Life. The Group Health Medical Associates," N. Engl. J. Med., **332**(3), pp. 133–138.
[46] Kouloumenta, V., Hatziefthimiou, A., Paraskeva, E., Gourgoulianis, K., and Molyvdas, P. A., 2006, "Non-Genomic Effect of Testosterone on Airway Smooth Muscle," Br. J. Pharmacol., **149**(8), pp. 1083–1091.
[47] Draijer, C., Hylkema, M. N., Boorsma, C. E., Klok, P. A., Robbe, P., Timens, W., Postma, D. S., Greene, C. M., and Melgert, B. N., 2016, "Sexual Maturation Protects Against Development of Lung Inflammation Through Estrogen," Am. J. Physiol. Lung Cell. Mol. Physiol., **310**(2), pp. L166–L174.
[48] Card, J. W., Voltz, J. W., Ferguson, C. D., Carey, M. A., DeGraff, L. M., Peddada, S. D., Morgan, D. L., and Zeldin, D. C., 2007, "Male Sex Hormones Promote Vagally Mediated Reflex Airway Responsiveness to Cholinergic Stimulation," Am. J. Physiol. Lung Cell. Mol. Physiol., **292**(4), pp. L908–L914.
[49] Lessey, E. C., Guilluy, C., and Burridge, K., 2012, "From Mechanical Force to RhoA Activation," Biochemistry, **51**(38), pp. 7420–7432.
[50] Tanaka, R., Al-Jamal, R., and Ludwig, M. S., 2001, "Maturational Changes in Extracellular Matrix and Lung Tissue Mechanics," J. Appl. Physiol., **91**(5), pp. 2314–2321.